Affinity of α-Actinin for Actin Determines the Structure and Mechanical Properties of Actin Filament Gels

Daniel H. Wachsstock,* William H. Schwarz,‡ and Thomas D. Pollard*
Departments of *Cell Biology and Anatomy and ‡Chemical Engineering, Johns Hopkins University, Baltimore, Maryland 21205 USA

ABSTRACT Proteins that cross-link actin filaments can either form bundles of parallel filaments or isotropic networks of individual filaments. We have found that mixtures of actin filaments with α-actinin purified from either *Acanthamoeba castellanii* or chicken smooth muscle can form bundles or isotropic networks depending on their concentration. Low concentrations of α-actinin and actin filaments form networks indistinguishable in electron micrographs from gels of actin alone. Higher concentrations of α-actinin and actin filaments form bundles. The threshold for bundling depends on the affinity of the α-actinin for actin. The complex of *Acanthamoeba* α-actinin with actin filaments has a K_d of 4.7 μM and a bundling threshold of 0.1 μM; chicken smooth muscle has a K_d of 0.6 μM and a bundling threshold of 1 μM. The physical properties of isotropic networks of cross-linked actin filaments are very different from a gel of bundles: the network behaves like a solid because each actin filament is part of a single structure that encompasses all the filaments. Bundles of filaments behave more like a very viscous fluid because each bundle, while very long and stiff, can slip past other bundles. We have developed a computer model that predicts the bundling threshold based on four variables: the length of the actin filaments, the affinity of the α-actinin for actin, and the concentrations of actin and α-actinin.

INTRODUCTION

Proteins that can bind more than one actin filament have traditionally been classified either bundling proteins or as network-forming proteins (e.g., Ref. 1). Bundles are arrays of parallel actin filaments, such as those in microvilli and stress fibers, while networks are isotropic gels of individual actin filaments, such as those seen in electron micrographs of the cell cortex (2). Some small, inflexible actin binding proteins such as the *Dictyostelium* 30,000-dalton protein (3) may be unable to form anything other than tightly packed bundles, and proteins that cross-link filaments at right angles such as macrophage ABP (4) may be unable to bundle. On the other hand, it seems unreasonable to us that a flexible molecule with actin binding sites at both ends, such as the spectrin superfamily (1) should be only able to do one or the other.

α-Actinin is a member of the spectrin superfamily of actin cross-linking proteins that is usually classified as a bundling protein (5). It is a dimer composed of two identical peptides of about 100 kDa each (6) that in electron micrographs appears as a rod 30–40 nm long (e.g., Ref. 7) with globular regions at each end. Based on the amino acid sequence and data from proteolysis experiments, the globular region is largely the amino terminus of the α-actinin monomer, and is the actin-binding domain (8) shared by many actin cross-linking proteins (1, 9). The rod consists of four repeats of a 120-amino acid motif similar to those of spectrin (10) and is slightly flexible (11). α-actinin serves as a good model for actin-cross-linking proteins because of its small size and abundance.

α-Actinins from vertebrate smooth muscle and *Acanthamoeba* are both calcium-insensitive actin cross-linkers (12), have similar shapes and sizes when bound to actin, and bundle actin filaments at high ratios of α-actinin to actin (5). *Acanthamoeba* α-actinin has a lower affinity for actin (5, 13) and increases the viscosity and rigidity of actin gels when deformed at high rates of shear. At low shear rates, amoeba α-actinin has little effect on the mechanical properties of actin (13). Sato et al. (13) postulated that these effects might be due to rapid rearrangement of the amoeba α-actinin cross-links, on a subsecond time scale, allowing slow deformations to relieve stress in the gel without breaking filaments.

An isotropic network of filaments has the mechanical properties of an elastic solid (14). Bundling of actin filaments changes the mechanical properties to that of a viscous fluid, with lower stiffness, because the bundles behave as long, thick rigid rods that can slip past one another (15). The tendency of α-actinin to bundle actin depends on the length of the filaments (16). In this study, we show that the bundling of actin filaments also depends on the concentration of cross-linker and the affinity of the cross-linker for actin filaments. The mechanical properties of isotropic networks of actin and α-actinin are very different from gels of bundles formed by the same proteins.

Received for publication 30 November 1992 and in final form 19 March 1993.

Address reprint requests to Daniel Wachsstock at the Department of Cell Biology and Anatomy, Wood Basic Science Bldg. 114, 725 N. Wolfe St., Baltimore, MD 21205.

0006-3495/93/07/205/10 $2.00

MATERIALS AND METHODS

Protein purification

Actin from rabbit skeletal muscle and α-actinin from *Acanthamoeba castellanii* were purified as described by Maciver et al. (16). α-Actinin from chicken smooth muscle was purified as described by Craig et al. (17). Both α-actinins were dialyzed into Buffer G (2 mM Tris, pH 8.0, 0.2 mM ATP,

0.1 mM $CaCl_2$, 0.5 mM dithiothreitol, 0.3 mM NaN_3) before use. Proteins were stored in Buffer G at 4°C and used within 1 week of purification.

Determination of binding constants

Varying concentrations of actin and of α-actinin were polymerized together in Buffer G with 0.1 mM KCl, 1 mM $MgCl_2$, and 0.5 mM EGTA at room temperature in 200-μl centrifuge tubes for 2 h. A 10-μl aliquot was removed, the remainder was centrifuged 1 h at 120,000 *g* in a Beckmann Airfuge, and 10 μl was removed from the meniscus. Uncentrifuged and supernatant samples were prepared for electrophoresis in sodium dodecyl sulfate on 10% polyacrylamide gels (18), stained with Coomassie Blue, and scanned in a Molecular Dynamics model 30E densitometer. The uncentrifuged samples were used to plot a standard curve to determine the free α-actinin concentration in the supernatant fractions. Free actin concentration was estimated as total actin − bound α-actinin. In any given experiment, either the actin or the α-actinin concentration was kept constant and used as the concentration of sites in the equilibrium binding equation, bound/sites = free/(K_d + free). The data were fit to this equation with the nonlinear least squares fitting program, Regression (Blackwell Scientific, Oxford).

Rheology

Quantitative physical measurements were made with an R18 cone and plate Weissenberg rheogoniometer (Sangamo Controls, Bognor Regis, Sussex, England) in the forced oscillation mode as described by Sato et al. (19). The amplitude of oscillations for all experiments was 8 μm, for a maximum shear strain of 1%. Protein samples were mixed and polymerization was initiated by adding 10 × polymerization buffer KME (final concentration, 2 mM Tris, pH 8.0, 50 mM KCl, 1 mM $MgCl_2$, 1 mM EGTA). The sample was immediately applied to the plates of the rheogoniometer and incubated overnight without shearing at 25°C in the instrument. The magnitude of the complex modulus, $|G^*|$, was calculated as $|G^*| = [G'^2 + (2\pi f \eta')^2]^{1/2}$ (20) where G' is the dynamic shear storage modulus, η' is the dynamic viscosity, and f is the frequency of oscillations in Hertz. The phase shift, δ, was calculated as $\tan \delta = 2\pi f \eta'/G'$. The magnitude of the complex modulus was reproducible to within a factor of 5 and the phase shift within 10% in three repetitions of the rheological experiments.

Electron microscopy

Samples were mixed and polymerized with KME in a volume of 100 μl in a porcelain tray and allowed to polymerize overnight at room temperature in a humidified chamber. They were fixed in situ, embedded, and sectioned as described in Maciver et al. (16).

Kinetics of polymerization

NBD-actin was made by the method of Detmers et al. (21) and was 100% labeled. Polymerization was measured by the fluorescence increase at 530 nm, with an excitation wavelength of 470 nm. Samples were mixed to a final volume of 1.08 ml in a plastic cuvette, and polymerization was initiated by adding 120 μl of 10 × KME. All reactions were kept at 25°C.

RESULTS

Binding of actin to α-actinin

We evaluated the binding of chicken and amoeba α-actinins to actin by a pelleting assay, estimating the concentration of α-actinin bound to actin from the concentration of free α-actinin in the supernatant (Fig. 1). Under the conditions used, α-actinin did not pellet alone, while virtually all the actin did (data not shown). At room temperature, amoeba α-actinin had a dissociation constant of 4.7 μM (Fig. 1 *C*), while chicken smooth muscle α-actinin had a dissociation constant of 0.6 μM (Fig. 1 *D*). These are similar to those reported by Meyer and Aebi (5). As both α-actinin molecules have similar sizes and shapes (5, 22), the association rate constants should be similar, and the 10-fold difference in equilibrium constants is likely due to a 10-fold greater dissociation rate constant for the amoeba α-actinin.

Rheology of actin/α-actinin gels

The magnitude of the complex modulus of a material measures its resistance to an oscillatory deformation as a function of the amplitude of deformation, while the phase shift between the deformation and the response depends on whether the material is solid or fluid. A solid will resist most when the deformation is maximal, and so the stress will be in phase with the deformation. A fluid will resist most when the rate of deformation is zero, so the phase shift is 90° or approximately 1.6 radians. All values for δ in this paper are given in radians.

For comparison, the modulus of steel is 7.6×10^{11} dyne/cm^2, with a phase shift of 0. The modulus of water ranges from 1.2×10^{-2} dyne/cm^2 at 0.19 Hz to 1.9×10^{-6} dyne/cm^2 at 0.0003 Hz, with a phase shift of 1.6 (20). Cross-linked long polymers are viscoelastic, with phase shifts between that of a solid and a fluid; highly cross-linked rubber has a phase shift of 0.2 with a modulus of about 10^8 dyne/cm^2.

Amoeba and chicken α-actinins differ both quantitatively and qualitatively in their effects on the mechanical properties of actin filament gels (Fig. 2). Actin filaments have a modulus that varies between 2 and 10 dynes/cm^2 depending on the frequency of deformation, with a phase shift about 0.3 radians (Fig. 2). As reported previously, (13, 16) amoeba α-actinin raises the modulus at high frequencies of deformation, with only a small effect at low frequencies. This was interpreted as an effect of a high dissociation rate constant. Actin networks cross-linked by α-actinin resist rapid deformations, but at low rates of deformation the networks are similar to actin filaments alone, since the cross-links can rearrange faster than the rate of filament displacement.

We used the approach of Brenner (23, 24) to interpret the rheological data in molecular terms. Brenner showed that a dynamically cross-linked polymer has a stiffness that depends on the velocity of deformation. The stiffness is similar to that of the uncross-linked material at very low speeds, while at high speeds it approaches that of a tightly cross-linked network. The stiffness is 50% of its maximum when time scale of the deformation is equal to $1/k_-$, the dissociation rate constant. With an oscillatory deformation, the dissociation constant should be approximately equal to the frequency of oscillation at half-maximal stiffness. The amoeba α-actinin/actin line was extrapolated back to the actin alone curve (the uncross-linked material) and forward to the chicken smooth muscle α-actinin curve (considered the tightly cross-linked material). The amoeba α-actinin reached 50% of the tightly cross-linked material's stiffness at a fre-

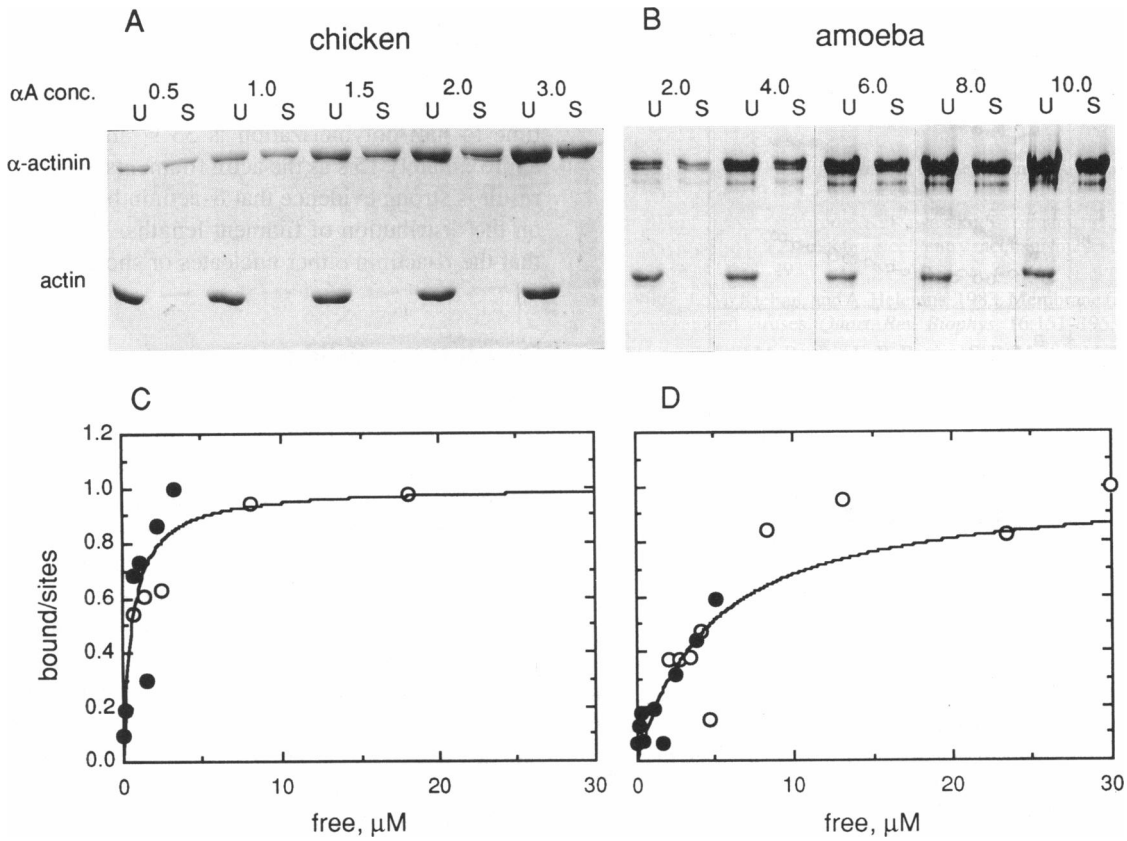

FIGURE 1 Pelleting assay to determine the dissociation equilibrium constant of actin and α-actinin. Proteins were polymerized together and centrifuged at 120,000 *g*. Identical aliquots of uncentrifuged (*U*) and supernatant (*S*) were run on a 10% gel and scanned as described under Materials and Methods. (*A*) 5 μM actin and varying chicken smooth muscle α-actinin. (*B*) 5 μM actin and varying amoeba α-actinin, which runs as a doublet (22). (*C*) Graph of bound/sites versus free protein for chicken smooth muscle α-actinin as described in the Materials and Methods. Open symbols are 5 μM actin with varying α-actinin. Closed symbols are 2 μM α-actinin with varying actin. Curve is the best fit to the data, with a K_d of 0.59 μM. (*D*) Graph of bound/sites versus free protein for amoeba α-actinin. Open symbols are 5 μM actin with varying α-actinin. Closed symbols are 2 μM α-actinin with varying actin. Curve is the best fit to the data, with a K_d of 4.73 μM.

quency of 3.2 Hz; thus the dissociation rate constant is approximately 3.2 s^{-1}. An equilibrium constant of 4.7 μM (Fig. 1 *D*) would give an association rate constant of 6.8×10^5 M^{-1} s^{-1}, consistent with a diffusion limited reaction. This analysis underestimates the true dissociation rate constant, since chicken α-actinin is not an infinitely tight cross-linker and thus does not represent the limiting stiffness at an infinitely rapid deformation. On the other hand, chicken smooth muscle α-actinin raises the modulus of actin filaments at all frequencies of deformation, consistent with a much lower dissociation rate and thus much more permanent bonds. The nearly constant increase makes it impossible to estimate the dissociation rate constant from these data, but if the association rate constant is the same as that of amoeba α-actinin, then the dissociation rate constant would be 0.37 s^{-1}.

The magnitude of the complex modulus and phase shift of mixtures of actin filaments with α-actinin depends on the concentration of α-actinin in a complex way that reveals a fundamental difference in the cross-linking properties of the two proteins (Fig. 3). At concentrations greater than a threshold of 0.4 μM, amoeba α-actinin increases the modulus and decreases the phase shift of actin filaments (Fig. 3), making the gel stiff and more solid-like. Chicken α-actinin differs in three ways: first, the threshold concentration for increasing the complex modulus is much lower, 0.02 μM. Second, at 0.1 μM α-actinin the complex modulus has a local maximum and at 1.0 μM there is a local minimum. At higher concentrations of chicken α-actinin the complex modulus increases to levels more than 20 times those with amoeba α-actinin. Third, at a chicken α-actinin concentration of 0.1 μM, when the magnitude of the complex modulus is at a local maximum, the phase shift is at a local minimum, between 0 and 0.1 at all frequencies (Fig. 3, *C* and *D*). Thus the chicken α-actinin/actin gel is very much like a solid at low α-actinin concentrations, while at higher concentrations it is more like a fluid. Amoeba α-actinin/actin gels are more fluid at all concentrations. This biphasic behavior indicates that the amoeba and the chicken smooth muscle α-actinins affect 15 μM actin gels differently between α-actinin concentrations of 0.1 and 1.0 μM.

Electron microscopy of actin/α-actinin gels

In the absence of α-actinin, solutions of actin filaments are homogeneous networks of randomly oriented individual filaments (Figs. 4 *A* and 5 *A*). The presence of low concen-

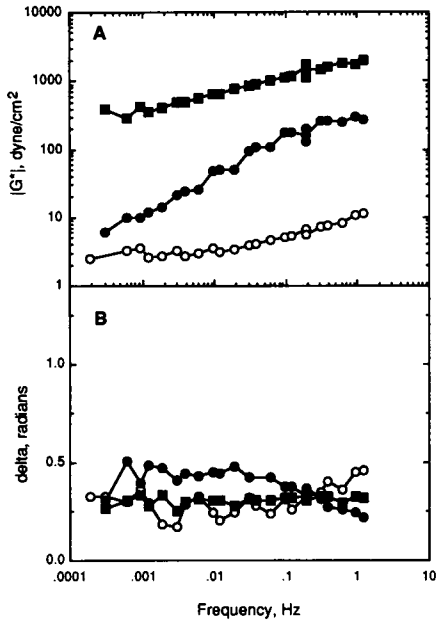

FIGURE 2 Rheological properties of actin filaments alone and with α-actinin as a function of frequency of deformation. 15 μM actin and 10 μM α-actinin were polymerized in the rheogoniometer. (*A*) Magnitude of the complex modulus for actin alone (○), actin with amoeba α-actinin (●), and actin with chicken α-actinin (■). The chicken α-actinin raises the modulus at all frequencies, while the amoeba α-actinin raises it only at high frequencies. (*B*) Phase shift of the complex modulus. A phase shift of 0 is typical of a solid; 1.6 is typical of a Newtonian fluid. At these concentrations, neither species of α-actinin has much influence on the phase shift of actin.

trations (0.1 μM) of α-actinin, whether chicken or amoeba, increases the stiffness of the gel 2–5-fold at high frequencies (0.2 Hz) (Fig. 3 *B*), but does not change the gross appearance of the network (Figs. 4 *B* and 5 *B*). A few small bundles are visible in the sample with amoeba α-actinin, while none are visible in the sample with chicken α-actinin; the α-actinin simply cross-links the existing network (compare to Pollard et al. (25)). It is possible that the distribution of filament orientations is affected by the presence of α-actinin, but there are no large bundles (compare Figs. 4 *D* and 5 *D*). It is this appearance that we call "isotropic."

At high concentrations (10 μM) of either α-actinin with 15 μM actin, all the actin filaments are aggregated into compact bundles (Figs. 4 *D* and 5 *D*). The center to center distance between filaments is approximately 8 nm. Electron dense material is visible between and around the filaments (Figs. 4 *D*, 5 *D*, and 6).

At intermediate concentrations, the two α-actinins differ. Amoeba α-actinin at a concentration of 1 μM aggregates actin filaments into bundles much like those seen at high α-actinin concentrations (Figs. 4 *C* and 6 *A*). These mixtures are fluid, with a phase shift greater than 0.2, as are all the amoeba α-actinin mixtures (Fig. 3). Chicken smooth muscle α-actinin does not bundle actin filaments until its concentration is very high (Fig. 5), while at concentrations up to the local minimum in the complex modulus at 1.0 μM (Fig. 3, *A* and *B*), the chicken α-actinin with actin retains the homogeneous networked appearance of actin alone.

Kinetics of polymerization

The presence of 1 μM of either α-actinin has no effect on the time course of polymerization of 15 μM actin (Fig. 7). The time to half-polymerization is 33 s, and there is a lag of approximately 15 s as the actin filaments are nucleated. This result is strong evidence that α-actinin has little or no effect on the distribution of filament lengths. It makes it unlikely that the α-actinin either nucleates or shortens the filaments.

Computer modeling

A relatively simple model can account for the dependence of the structure of the mixtures of actin filaments and α-actinin on the concentration of α-actinin (Appendix and Fig. 8). In particular, this model predicts quantitatively the concentrations of the two different α-actinins required for the transition from an isotropic gel to bundles of filaments.

The model assumes that diffusion and reversible molecular interactions alone account for the structure of the actin filament assemblies. Thus the only four variables are the concentrations of actin and α-actinin, the length of the actin filaments, and the affinity of the α-actinin for the actin filaments, and there are no arbitrary parameters used to fit the data. Since our experiments have been done on samples where the actin filaments polymerized from monomers in the presence of α-actinin, the concentration and length of the filaments is varied with time during the calculations. The computer uses this model and the four variables to calculate binding and orientation of two filaments relative to each other as test of the tendency of the whole ensemble of filaments in a bulk sample to align in bundles.

The model predicts that the filaments will form random networks at low concentrations of gizzard α-actinin and bundles at concentrations above 1 μM α-actinin (Fig. 8), exactly as observed. The concentration of amoeba α-actinin required for bundling is 0.1 μM (Fig. 8), as observed. Assuming a K_d of 2 μM, the model also fits the data reported by Hou et al. (26) for bundling of actin filaments by filamin (Fig. 9). The model predicts a bundling threshold at a ratio of 1 filamin/163 actins, close to the observed value of 1/140.

DISCUSSION

Early thoughts about the effects of protein cross-linkers on the structure and mechanical properties of actin filament networks have been relatively simple, assuming that the cross-linked filaments are a viscoelastic material with a stiffness that depends more or less directly on the density of the cross-links. Furthermore, many authors have argued that the structure of these gels depends on the particular cross-linking protein, with some having a strong tendency to form isotropic gels and others favoring bundles of filaments (see Ref 1). Recent work has suggested that the situation is more complex with mixtures of actin and a given cross-linker forming either isotropic networks or bundles depending on the concentrations of the proteins (16, 26) and the length of the filaments (16, 27).

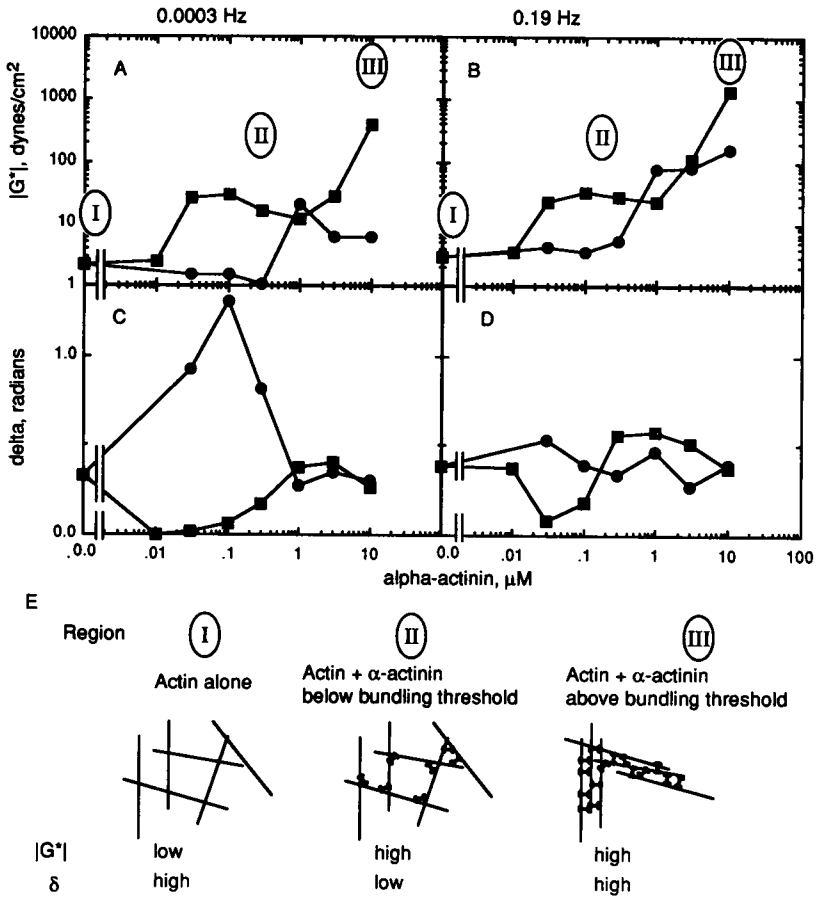

FIGURE 3 Dependence of the rheological properties of actin filaments on the concentration of α-actinin at two frequencies of deformation. Mixtures of 15 μM actin and varying concentrations of α-actinin were polymerized in the rheogoniometer and moduli were measured at all frequencies, two extremes of which are shown. Circles indicate amoeba α-actinin and squares indicate chicken α-actinin. *A* and *B* represent magnitude of the complex modulus, $|G^*|$ (*C*) and *D* represent phase shift, δ. *A* and *C* are at 0.0003 Hz; *B* and *D* are at 0.19 Hz. (*E*) Schematic drawing of the structure of actin/α-actinin gels. Compare to Figs. 4 and 5. Thin lines represent actin filaments; the dumbbell shapes represent α-actinin and are not to scale. Also shown are the expected magnitudes of the rheological parameters. Regions I, II, and III correspond approximately to the similarly marked regions in the graphs. Note that the threshold differs for chicken and amoeba α-actinin.

Here we report that both the structure and mechanical properties of mixtures of actin filaments and α-actinin depend in a complicated way on both the concentration and affinity of this cross-linking protein for actin. At low concentrations of α-actinin the gel is isotropic and the elastic modulus depends directly on the concentration of the cross-linker as expected from theoretical considerations (14). Compared with actin filaments alone, the mixtures behave more as a solid with a higher complex modulus and a lower phase shift. At intermediate concentrations of cross-linker, the complex modulus falls and the phase shift rises. By electron microscopy the actin filaments appear to be random. At high concentrations of α-actinin, the filaments aggregate into bundles. The complex modulus again varies directly with the concentration of α-actinin, but the phase shift declines to about 0.2, a value closer to that of a fluid rather than the solid observed at low concentrations of cross-linker. The concentration of α-actinin required for the transition from an isotropic viscoelastic solid to a viscous fluid of actin bundles depends on the affinity of the α-actinin for actin. In our examples, the transition concentration for low affinity amoeba α-actinin was about 10 times smaller than for the higher affinity smooth muscle α-actinin.

Although these phenomena appear to be complex, a relatively simple model with four variables (concentrations of actin and cross-linker, length of the filaments, and affinity of the cross-linker) and minimal assumptions can account for both our data and that of others (Figs. 8 and 9). The details regarding the computations are found in the Appendix. Here we focus on the mechanisms that explain how the concentration and affinity of α-actinin affects the structure and mechanical properties of the actin filaments.

At the actin concentrations used in our experiments, actin polymerizes into random networks (28) unless a favorable combination of cross-linker and polymer length exist to promote bundle formation. The polymer length is an important variable since formation of a bundle requires the alignment of filaments. Long filaments will be entangled and less able to rearrange by diffusion into bundles. The affinity of the cross-linker is an issue, because the rate of dissociation will determine whether filaments can realign into bundles. Tight cross-linkers will freeze the filaments in an isotropic network, so the bundling threshold is higher for cross-linkers that bind tightly.

When the filaments are short, they diffuse freely and have few α-actinin molecules bound, so diffusion keeps them randomly oriented. As they become longer, they bind more α-actinin and become frozen in position. If the affinity for actin is low, then the α-actinin will dissociate and allow the filaments to continue diffusing. If the filaments, with many α-actinin molecules bound, diffuse to a position where they are close to parallel, many of the α-actinin molecules will cross-link the filaments, so that even if one dissociates, the others will keep the filaments aligned. Thus, once bundles

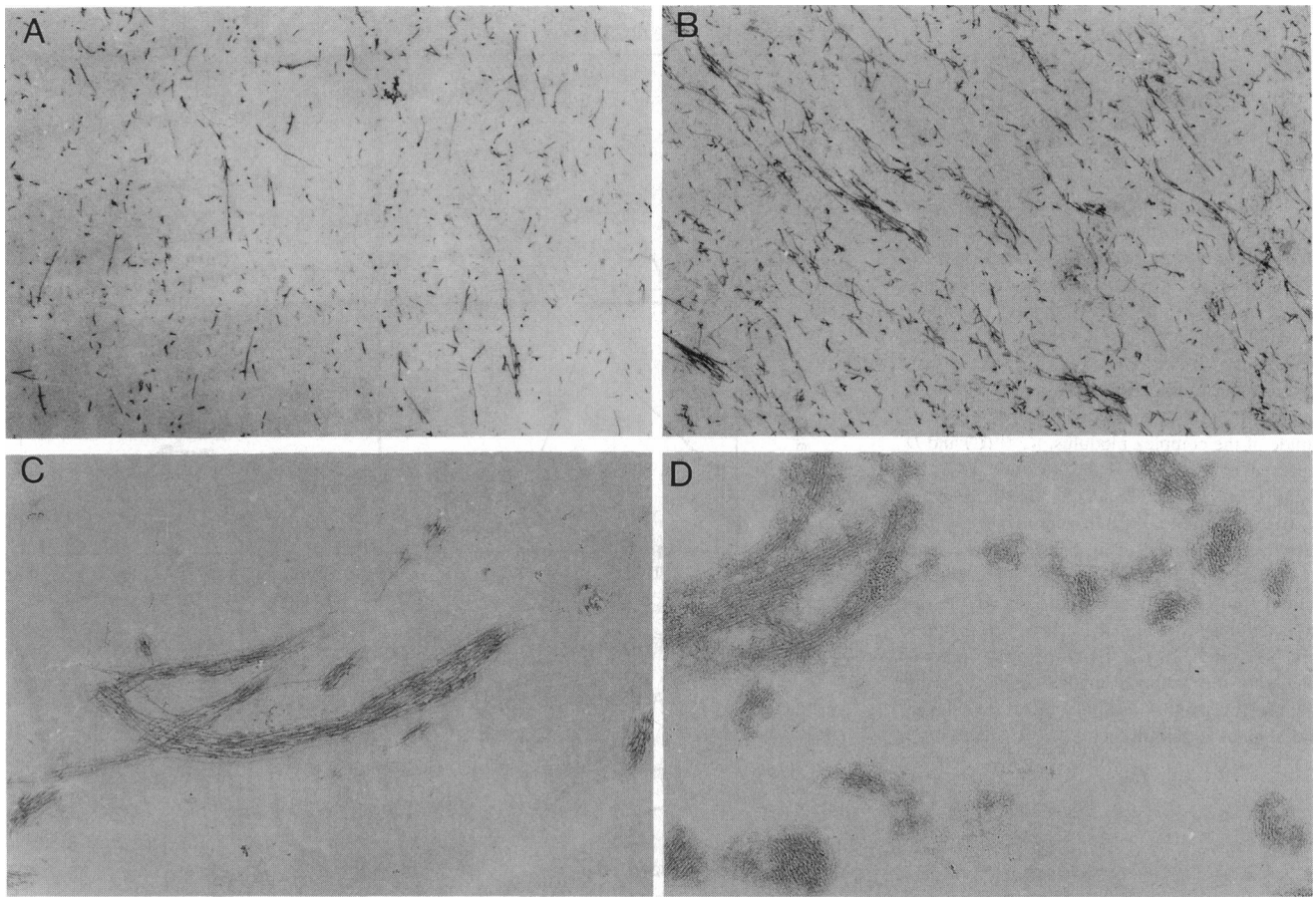

FIGURE 4 Electron micrographs of thin sections of mixtures of actin filaments and amoeba α-actinin at 20,000 × magnification. (*A*) 15 μM actin alone. (*B*) Actin with 0.1 μM α-actinin. (*C*) Actin with 1 μM α-actinin. (*D*) Actin with 10 μM α-actinin. A few small bundles are visible at 0.1 μM α-actinin, while large bundles are evident at higher concentrations.

form they tend not to reform isotropic networks. The transition from isotropic network to bundles is not a true phase shift, but a kinetically limited reaction.

At concentrations of α-actinin less than the bundling threshold, the gel is cross-linked in proportion to the α-actinin concentration without changing its isotropic nature (Figs. 4 and 5). The extent of cross-linking determines the elastic component of the modulus (14). More extensive cross-linking results in a higher complex modulus and a lower phase shift (i.e., a more solid-like material).

At threshold concentrations of α-actinin, the actin filaments begin to bundle. We propose that the modulus is less than that of an isotropic gel, and the phase shift is greater, because the incipient bundles are able to slip past one another and the gel is more fluid (Fig. 3). In electron micrographs, the filaments in the gels can still appear largely homogeneous, with a few small bundles visible (Figs. 4 and 5).

At concentrations of α-actinin above the threshold, the actin filaments form bundles that are obvious in the electron microscope (Figs. 4–6). As more filaments are recruited into the bundles, the complex modulus, or the stiffness, of the gel increases. These bundles may be somewhat cross-linked to each other, but will still be largely able to slip past one another, so the phase shift is closer to that of a fluid than the isotropic network—about 0.2.

This triphasic behavior is most obvious with the chicken smooth muscle α-actinin, which has a bundling threshold around 1 μM (as predicted from theory in Fig. 8). There is a maximum in the phase shift and a minimum in the modulus at 1 μM, and bundling is evident at α-actinin concentrations greater than 1 μM.

The data with amoeba α-actinin are harder to interpret, for two reasons. First, owing to its low affinity for actin, the amoeba α-actinin has a very small effect on the mechanical properties at low frequencies, especially at low concentrations. Consequently, Figs. 3 *A* and 3 *C* show no effect of amoeba α-actinin in the range of concentrations where the model predicts isotropic gel formation, because the frequency of deformation is low. For the same reason, it is difficult to observe a clear minimum in the modulus at the bundling threshold, although the micrographs (Fig. 4) and the local maximum in the phase shift between 0.1 and 0.03 μM (Fig. 3) indicate that the bundling threshold is about 0.1 μM, as predicted by theory (Fig. 8).

Hou et al. (26) have also observed the transition of actin filament gels from networks to bundles with the cross-linking

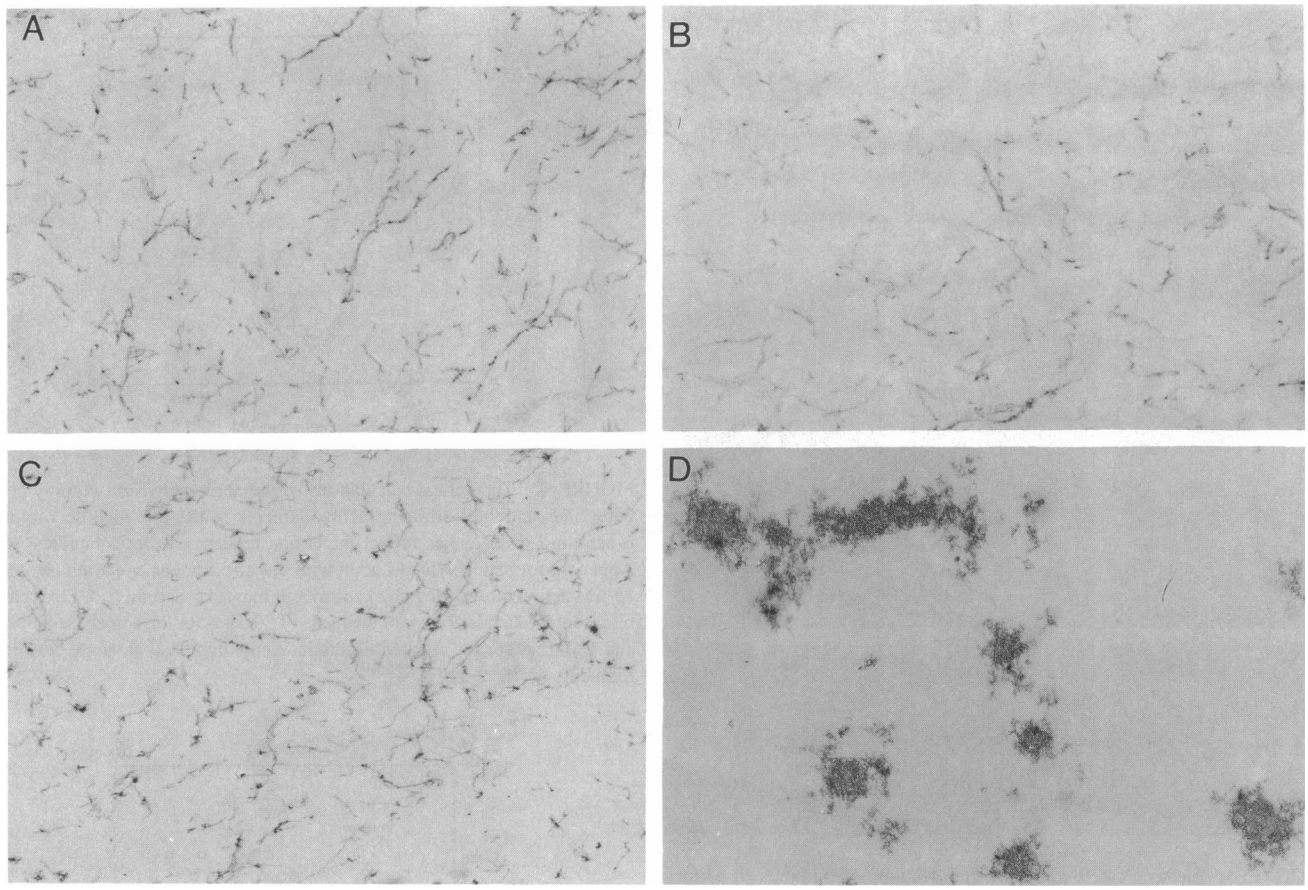

FIGURE 5 Electron micrographs of thin sections of mixtures of actin filaments and chicken α-actinin at 20,000 × magnification. (*A*) 15 μM actin alone. (*B*) Actin with 0.1 μM α-actinin. (*C*) Actin with 1 μM α-actinin. (*D*) Actin with 10 μM α-actinin. A few small bundles are visible at 1 μM α-actinin, while large bundles are evident at higher concentrations.

protein filamin. They documented the transition by light microscopy and fluorescence photobleaching recovery, but did not relate the structure of the gel to the mechanical properties. They varied the actin concentration over a wide range, and found the bundling threshold at a filamin concentration 1/140 of the actin concentration. Using the model presented here and a mean filamin length of 100 nm (29) we found the best fit to their data with a K_d of 2 μM and a bundling threshold at a filamin concentration 1/163 of the actin concentration (Fig. 9).

Simon et al. (30) found that high concentrations of *Dictyostelium* α-actinin with fluorescently labeled F-actin formed inhomogenous domains on the order of 100 μm. The threshold they found, 0.1 μM α-actinin with 12 μM actin, is consistent with our model and a K_d of 3 μM (5). Grazi et al. (31) found that the concentration of rabbit skeletal muscle α-actinin had a complex effect on the low shear viscosity of low concentrations of actin (1.2 μM). Concentrations of α-actinin up to 0.5 nM increased the viscosity; between 0.5 and 1 nM α-actinin lowered the viscosity; beyond this the viscosity increased directly with the concentration of α-actinin. They describe electron micrographs of their actin gels, with bundles forming predominantly above an α-actinin to actin ratio of 1 to 6. Brown (32) also found that the formation of bundles with low concentrations of actin (4.1 μM) decreased the viscosity. These observations are consistent with the model that predicts that bundling will decrease actin gel viscosity as bundles slip past each other.

It seems clear that the structure of actin gels depends in a complex fashion on the composition of the sample and kinetics of its assembly. In our experiments the actin was polymerized in the presence of cross-linkers, so the filaments are initially short and able to form bundles. In the cell, most filaments are less than 1 μm long (33–35), considerably shorter than those formed in vitro (36, 37). Short filaments can rearrange and form bundles far more readily than long ones (16), so actin filament severing and capping proteins that regulate filament length could rapidly change the physical properties of the cell.

Both actin cross-linking proteins used in this study are calcium-insensitive (12, 38), but most nonmuscle α-actinins are calcium-sensitive (38). Cells with these α-actinins may regulate actin filament cross-linking by varying the calcium concentration, in effect turning amoeba α-actinin into smooth muscle α-actinin. This will affect both the extent of cross-linking, the arrangement of the filaments and the mechanical properties. As shown here, these effects could be counterintuitive: lowering the affinity can increase the ten-

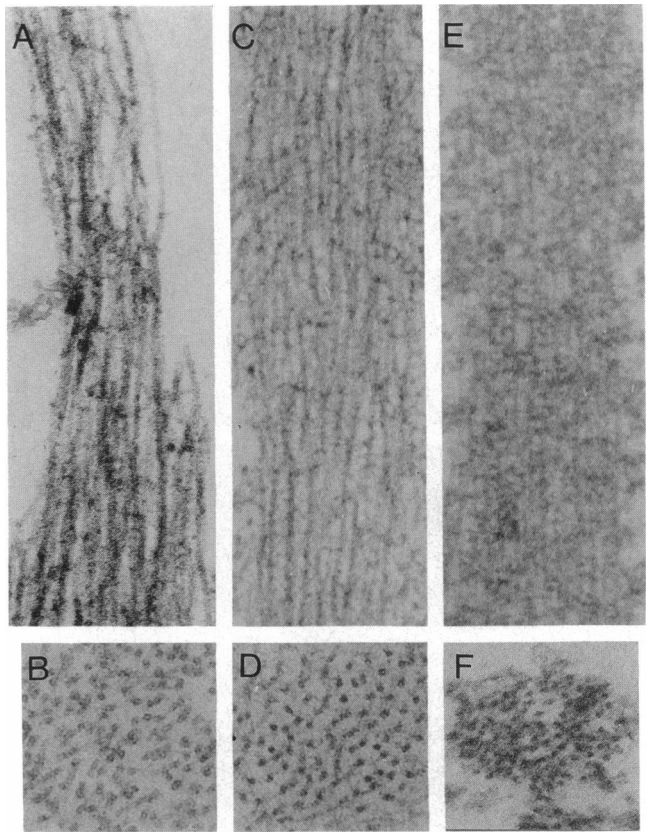

FIGURE 6 Electron micrographs of thin sections of mixtures of actin filaments and α-actinin, showing bundles in greater detail. Shown are typical bundles, all 100,000 × magnification. *A* and *B* represent 15 μM actin with 1 μM amoeba α-actinin. *C* and *D* represent actin with 10 μM amoeba α-actinin. *E* and *F* represent actin with 10 μM chicken α-actinin. *A*, *C*, and *E* represent longitudinal sections. *B*, *D*, and *F* represent cross sections. Bundles all have approximately 8-nm spacing between actin filaments, and increasing α-actinin shows increasing electron-dense material between filaments.

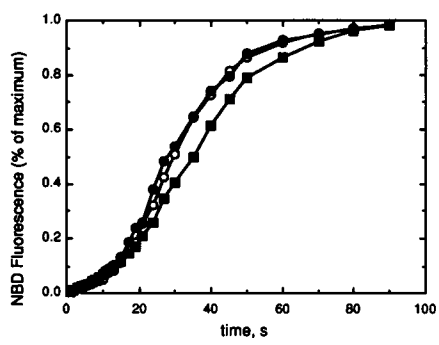

FIGURE 7 Time course of actin polymerization, measured by NBD-actin fluorescence at 530 nm. Shown are 15 μM actin alone (○), actin with 1 μM amoeba α-actinin (■), and actin with 1 μM chicken α-actinin (●).

dency of filaments to form bundles and increase the stiffness of the cytoplasm (cf. Fig. 3 at 1 μM α-actinin). Variation of the affinity of a major cross-linking protein like α-actinin could also dramatically alter the physical properties of cytoplasm by changing its structure as described here.

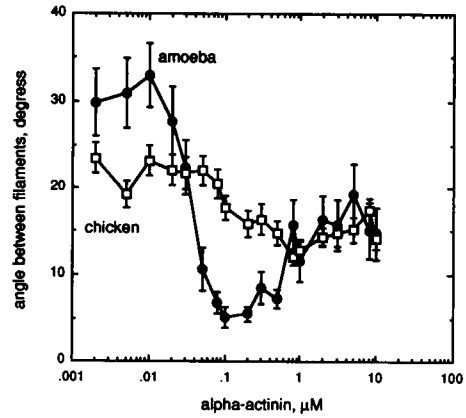

FIGURE 8 Theoretical calculations of the angle between two polymerizing and randomly diffusing actin filaments in the presence of varying α-actinin. Lower angles reflect increasing tendency to form bundles; see Appendix for details. 15 μM actin with varying amoeba α-actinin (●) and 15 μM actin with varying chicken smooth muscle α-actinin (□). Error bars represent the standard error of the mean of 50 trials for the amoeba α-actinin and 100 trials for the chicken α-actinin. Actin alone had an angle between filaments of 45 ± 5°.

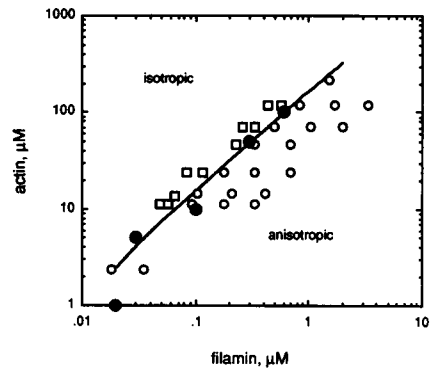

FIGURE 9 Calculated bundling threshold for mixtures of actin filaments and filamin, compared to data of Hou et al. (26). Hou et al. determined the structure of actin/filamin gels at varying concentrations by differential interference contrast microscopy. They rated the samples as isotropic (□) or anisotropic (○). ●, the bundling threshold for various concentrations of actin, calculated using the model described in the Appendix, assuming an equilibrium dissociation constant of 2 μM and a cross-linker length of 100 μM. The solid line is the linear least-squares fit through the calculated points, with a filamin:actin ratio of 1:163.

We propose that the distinction between the cross-linking proteins that either promote the formation of networks or bundle actin filaments is artificial; many if not all of these cross-linking proteins are probably capable of either, depending on the conditions of polymerization and the relative rates of cross-linking and reorganization of the filaments. At concentrations of cross-linker lower than a bundling threshold, the filaments form an isotropic network. The greater the affinity of the cross-linking protein for actin filaments, the higher this threshold, as the filaments are less able to rearrange into bundles.

APPENDIX

We developed a computer model (available from Daniel Wachsstock) to predict the bundling threshold for mixtures of actin and a cross-linking protein. The model was run on a Macintosh IIci computer, and took 30 min for each 50-simulation run.

The model uses two actin filaments that can diffuse relative to one another, with the diffusion constants given by Doi and Edwards (39) for a rigid rod. The actin filaments are modeled as simple rigid rods of length L and width b, 8 nm (40). We simplified the model by assuming the filaments were rotationally symmetrical, ignoring the helical nature of the actual actin filament. The filaments began at a distance of $d_f = \nu^{1/3}$ apart, where ν is the concentration of filaments, which is $C_a/(370L_f)$. L_f is the mean length of the actin filaments, 4.9 μm (37), and 370 is the number of actin subunits per μm of filament. d_f thus represents the mean interfilament spacing. The filaments began perpendicular to each other, in the same plane.

The translational diffusion constant for motion perpendicular to the axis is:

$$D_{t,perp} = \frac{kT \ln(L/b)}{\pi\eta L} \quad (1)$$

where k is Boltzmann's constant, T is the absolute temperature, and η is the viscosity of water.

The translational diffusion constant for motion parallel to the axis is as follows.

$$D_{t,par} = \frac{D_{t,perp}}{2} \quad (2)$$

The rotational diffusion constant is as follows.

$$D_r = \frac{kT[\ln(L/b) - 0.8]}{\pi\eta L^3} \quad (3)$$

Under conditions where the actin polymerizes in the presence of the cross-linker, the length of the filament varies with time; to simplify the model we assumed that all the filaments grew identically and used the mean filament length L_f as the final length. The kinetics of growth were taken from the data in Fig. 7.

The model calculated the position in three dimensions of each filament after time steps of Δt, usually 0.01 s. At each step, the filaments grew to the appropriate length and diffused, and α-actinin molecules bound to and dissociated from the filaments. If any α-actinin molecules remained bound to both filaments, then on the next cycle the filaments could not translate relative to one another and rotational diffusion was limited, so the distance between filaments at the point where the α-actinin bound was less than l_α, the length of the α-actinin, or 36 nm (7). If a filament was bound to an α-actinin molecule on a distant filament (as described below) it did not diffuse at all on the next cycle.

The diffusion was performed using toroidal boundary conditions: if a filament diffused more than the mean interfilament spacing, d_f, away from the other, the filament was displaced to d_f away on the other side. This simulates the presence of other filaments in the system that can diffuse in. It is a simplification in that it does not allow for three or more filaments at once.

The algorithm for calculating α-actinin binding was as follows: the concentration of α-actinin bound to at least one actin filament, C_b, is the solution of the equilibrium equation:

$$\frac{(C_a - C_b)(C_\alpha - C_b)}{C_b} = K_d, \quad (4)$$

where C_a is the concentration of actin incorporated into filaments, which is known from the initial concentration of actin and the kinetics of polymerization; C_α is the total concentration of α-actinin, and K_d is the equilibrium dissociation constant, which is known from the data in Fig. 1. The number of α-actinin molecules bound to a single filament is C_b/ν. This number of α-actinin molecules bound randomly along the filament.

Any α-actinin molecule that was bound to only one filament but was within l_α of the other filament bound to that other filament. Any α-actinin molecule that was bound to both filaments dissociated from one of them with a rate $k_- = K_d/k_+$, where k_+ is the association rate constant estimated to be $6.8 \times 10^5\ M^{-1}\ s^{-1}$ (see text and Fig. 2). To simulate the random dissociation, each α-actinin dissociated with a probability $\Delta t\ k_-$.

Also on each cycle, the filaments were allowed to bind to α-actinin molecules bound to filaments other than the two being simulated. The probability of an α-actinin molecule being within l_α of a filament of length L is the concentration of bound α-actinin times the volume of the cylinder around the filament, or

$$\text{prob} = \pi l_\alpha^2 L C_b. \quad (5)$$

Once bound, these distant α-actinin molecules dissociated as described above.

This algorithm was repeated until the filaments reached the semidilute limit, beyond which the diffusion of the filaments becomes severely limited (39). The limit is equal to d_f. Each simulation was run at least 50 times, and the mean final angle between the filaments was reported as a measure of bundling. Small angles reflect bundling, while angles closer to 45° reflect an isotropic distribution. This algorithm was repeated for a series of α-actinin concentrations at a constant actin concentration, and the α-actinin concentration with the minimum mean angle was defined as the bundling threshold (Fig. 8).

The purpose of the model is to estimate the bundling threshold, not the steady state orientation of the filaments. The model involves only two filaments interacting. In the actual experiments that involve many filaments, the bundling is cooperative. As more filaments are incorporated into bundles, it becomes easier for additional filaments to align (28). Once two filaments are bundled, they will move together and are able to bundle with other filaments. Thus in the experiments, the bundling threshold is much more dramatic and tends to be an all-or-none phenomenon. In the electron micrographs (Figs. 4 and 5), the filaments are either bundled or not, whereas the model has a more gentle slope in the angle between filaments.

This model assumes that the actin filaments are rigid rods. This is a simplification that makes the mathematics tractable. In fact, actin filaments have a persistence length of 12.5 μm (37), so the ends of a 4.9-μm filament would have a mean angular deviation of 47°. This flexibility of the filaments affects the rheological parameters of cross-linked gels but probably not the propensity to form bundles, which depends on the rate of cross-linking and the diffusion of the filaments as a whole.

We gratefully acknowledge Pamela Maupin for assisting with the electron microscopy and Joan Richstmeier for the use of her computing facilities. This work was supported by National Institutes of Health grant GM-26338 (to T. D. Pollard). D. H. Wachsstock was supported by the Medical Scientist Training Program (grant GM-07309).

REFERENCES

1. Matsudaira, P. 1991. Modular organization of actin cross-linking proteins. *Trends Biol. Sci.* 16:87–92.
2. Stossel, T. P. 1983. The spatial organization of cortical cytoplasm in macrophages. *In* Spatial Organization of Eukaryotic Cells. J. R. McIntosh, editor. Alan R. Liss, New York. 203–223.
3. Fechheimer, M., and D. L. Taylor. 1984. Isolation and characterization of a 30,000-dalton calcium-sensitive actin cross-linking protein from *Dictyostelium discoideum*. *J. Biol. Chem.* 259:4515–4520.
4. Niederman, R., P. C. Amrein, and J. Hartwig. 1983. Three-dimensional structure of actin filaments and of an actin gel made with actin binding protein. *J. Cell Biol.* 96:1400–1413.
5. Meyer, R. K., and U. Aebi. 1990. Bundling of actin filaments by alpha-actinin depends on its molecular weight. *J. Cell Biol.* 110:2013–2024.
6. Suzuki, A., D. E. Goll, M. H. Stromer, I. Singh, and J. Temple. 1973. Alpha-actinin from red and white porcine muscle. *Biochim. Biophys. Acta.* 295:188–207.
7. Podlubnaya, Z. A., L. A. Tskhovrebova, M. M. Zaalishvili, and G. A.

Stephanenko. 1975. Electron microscopic study of alpha-actinin. *J. Mol. Biol.* 92:357–359.

8. Mimura, N., and A. Asano. 1986. Isolation and characterization of a conserved actin-binding domain from rat hepatic actinogelin, rat skeletal muscle and chicken gizzard alpha-actinins. *J. Biol. Chem.* 261: 10680–10687.
9. Bresnick, A. P., V. Warren, and J. Condeelis. 1990. Identification of a short sequence essential for actin binding by *Dictyostelium* ABP-120. *J. Biol. Chem.* 265:9236–9240.
10. Blanchard, A., V. Ohanian, and D. Critchley. 1989. The structure and function of alpha-actinin. *J. Muscle Res. Cell Motil.* 10:280–289.
11. Kahana, E., and W. B. Gratzer. 1991. Properties of the spectrin-like structural element of smooth-muscle alpha-actinin. *Cell Motility Cytoskel.* 20:242–248.
12. Pollard, T. D. 1986. Assembly and dynamics of the actin filament system in nonmuscle cells. *J. Cell. Biochem.* 31:87–95.
13. Sato, M., W. H. Schwarz, and T. D. Pollard. 1987. Dependence of the mechanical properties of actin/α-actinin gels on deformation rate. *Nature.* 325:828–830.
14. Nossal, R. 1988. On the elasticity of cytoskeletal networks. *Biophys. J.* 53:349–359.
15. Jockusch, B., and G. Isenberg. 1981. Interaction of alpha-actinin and vinculin: opposite effects on filament network formation. *Proc. Natl. Acad. Sci. USA.* 78:3005–3009.
16. Maciver, S. K., D. H. Wachsstock, W. H. Schwarz, and T. D. Pollard. 1991. The actin filament severing protein actophorin promotes the formation of rigid bundles of actin filaments cross-linked with alpha-actinin. *J. Cell Biol.* 115:1621–1628.
17. Craig, S. W., C. L. Lancashire, and J. A. Cooper. 1982. Preparation of smooth muscle alpha-actinin. *Methods Enzymol.* 85:316–321.
18. Laemmli, U. K. 1970. Cleavage of structural proteins during the assembly of the head of bacteriophage T4. *Nature.* 227:680–685.
19. Sato, M., G. Leimbach, W. H. Schwarz, and T. D. Pollard. 1985. Mechanical properties of actin. *J. Biol. Chem.* 260:8585–8592.
20. Ferry, J. D. 1980. Viscoelastic Properties of Polymers. John Wiley & Sons, New York. 641 pp.
21. Detmers, P., A. Weber, M. Elzinga, and R. E. Stephens. 1981. 7-Chloro-4-nitrobenzeno-2-oxa-1,3-diazole actin as a probe for actin polymerization. *J. Biol. Chem.* 256:99–105.
22. Pollard, T. D., P. C.-H. Tseng, D. L. Rimm, D. P. Bichell, R. C. Williams, J. Sinard, and M. Sato. 1986. Characterization of alpha-actinin from *Acanthamoeba. Cell Motil. Cytoskel.* 6:649–661.
23. Brenner, B. 1989. Muscle mechanics and biochemical kinetics. *In* Molecular Mechanisms in Muscular Contraction. J. M. Squire, editor. Macmillian, New York. 77–149.
24. Brenner, B. 1991. Rapid dissociation and reassociation of actomyosin cross-bridges during force generation: a newly observed facet of cross-bridge actin in muscle. *Proc. Natl. Acad. Sci. USA.* 88:10490–10494.
25. Pollard, T. D., U. Aebi, J. A. Cooper, M. Elzinga, W. E. Fowler, L. M. Griffith, I. M. Herman, J. Heuser, G. Isenberg, D. P. Kiehart, J. Levy, S. MacLean-Fletcher, P. Maupin, M. S. Mooseker, M. Runge, P. R. Smith, and P. Tseng. 1982. The mechanism of actin-filament assembly and cross-linking. *In* Cell and Muscle Motility. R. M. Dowben, and J. W. Shay, editors. Plenum Publishing Corp., New York. 15–44.
26. Hou, L., K. Luby-Phelps, and F. Lanni. 1990. Brownian motion of inert tracer macromolecules in polymerized and spontaneously bundled mixtures of actin and filamin. *J. Cell Biol.* 110:1645–1654.
27. Cortese, J. D., and C. Frieden. 1990. Effect of filamin and controlled linear shear on the microheterogeneity of F-actin/gelsolin gels. *Cell Motil. Cytoskel.* 17:236–249.
28. Coppin, C. M., and P. C. Leavis. 1992. Quantitation of liquid-crystalline ordering in F-actin solutions. *Biophys. J.* 63:794–807.
29. Gorlin, J. B., R. Yamin, S. Egan, M. Stewart, T. P. Stossel, D. J. Kwiatkowski, and J. Harwig. 1990. Human endothelial actin-binding protein (ABP-280, nonmuscle filamin): A molecular leaf spring. *J. Cell Biol.* 111:1089–1105.
30. Simon, J. A., R. H. Furukawa, B. R. Ware, and D. L. Taylor. 1988. The molecular mobility of alpha-actinin and actin in a reconstituted model of gelation. *Cell Motil. Cytoskel.* 11:64–82.
31. Grazi, E., G. Trombetta, and M. Guidoboni. 1991. Binding of alpha-actinin to F-actin or to tropomyosin F-actin is a function of both alpha-actinin concentration and gel structure. *J. Muscle Res. Cell Motil.* 12: 579–584.
32. Brown, S. S. 1985. A Ca^{2+}-insensitive actin-cross-linking protein from *Dictyostelium discoideum. Cell Motil.* 5:529–543.
33. Small, J. V. 1981. Organization of α-actinin in the leading edge of cultured cells: influence of osmium tetroxide and dehydration on the ultrastructure of actin meshworks. *J. Cell Biol.* 91:695–705.
34. Podolski, J. L., and T. L. Steck. 1990. Length distribution of F-actin in *Dictyostelium discoideum. J. Biol. Chem.* 265:1312–1318.
35. Cano, M. L., D. A. Lauffenburger, and S. H. Zigmond. 1991. Kinetic analysis of F-actin depolymerization in polymorphonuclear leukocyte lysates indicates that chemoattractant stimulation increases actin filament number without altering the filament distribution. *J. Cell Biol.* 115:677–687.
36. Lanni, F., and B. R. Ware. 1984. Detection and characterization of actin monomers, oligomers, and filaments in solution by measurement of fluorescent photobleaching recovery. *Biophys. J.* 46:97–110.
37. Burlacu, S., P. A. Janmey, and J. Borjedo. 1992. Distribution of actin filament lengths measured by fluorescence microscopy. *Am. J. Physiol.* 262:C569-C577.
38. Burridge, K., and J. R. Feramisco. 1981. Non-muscle alpha-actinins are calcium-sensitive actin-binding proteins. *Nature.* 294:565–567.
39. Doi, M., and S. F. Edwards. 1986. The Theory of Polymer Dynamics. Clarendon Press, Oxford. 391 pp.
40. Bremer, A., R. C. Millonig, R. Sütterlin, A. Engel, T. D. Pollard, and U. Aebi. 1991. The structural basis for the intrinsic disorder of the actin filament:The "lateral slipping" model. *J. Cell Biol.* 115:689–703.